



## MATHEMATICAL MODEL FOR DIRECT EVAPORATIVE SPACE COOLING SYSTEMS

M. C. Ndukwu<sup>1</sup>, S.I. Manuwa<sup>2</sup>, O. J. Olukunle<sup>3</sup>, I.B. Oluwalana<sup>4</sup>

<sup>1</sup>DEPT OF AGRICULTURAL AND BIO-RESOURCES ENG'G, MICHAEL OKPARA UNIV. OF AGRICULTURE UMUDIKE, NIGERIA.

<sup>2,3</sup>DEPT. OF AGRICULTURAL ENGINEERING, FEDERAL UNIVERSITY OF TECHNOLOGY AKURE, P.M.B. 704 AKURE, NIGERIA.

<sup>4</sup>DEPT. OF FOOD SCIENCE AND TECHNOLOGY, FEDERAL UNIV. OF TECHNOLOGY AKURE, P.M.B. 704 AKURE, NIGERIA.

E-mail addresses: <sup>1</sup>[ndukwumcu@gmail.com](mailto:ndukwumcu@gmail.com); <sup>2</sup>[manuwaseth@rocketmail.com](mailto:manuwaseth@rocketmail.com), <sup>3</sup>[wale\\_olukunle@yahoo.com](mailto:wale_olukunle@yahoo.com), <sup>4</sup>[ioluwalana2002@yahoo.com](mailto:ioluwalana2002@yahoo.com)

### Abstract

*This paper deals with the development of a simple mathematical model for experimental validation of the performance of a small evaporative cooling system in a tropical climate. It also presents the coefficient of convective heat transfer of wide range of temperatures based on existing model. Extensive experiments have been performed during January to February 2013 for a small evaporative cooling system designed for storage of fruits and vegetables. The model considered the thermal properties of the material of the cooling pad and assumed that the cooling pad is a plain porous wall bounded by two convective air at different temperature at the two surfaces. The predicted and experimental value of various cooling efficiency at different range of inlet temperature has been determined. In addition the values of the coefficient of convective heat transfer for a wide range of temperatures is also presented.*

**Keywords:** evaporative cooling, cooling pad, model equation, heat transfer

### 1. Introduction

The basic principle of evaporative cooling is cooling by evaporation. When water evaporates, it draws energy from its surroundings, which produces a considerable cooling effect. Evaporative cooling occurs when air, that is not too humid, passes over a wet surface (humidifier). The movement of the air can be passive i.e. when the air flows naturally through the pads or active with fans or blowers. The driving force for heat and mass transfer between air and water is the temperature and partial vapor pressure differences. Water is the working fluid in evaporative cooling thus it is environmentally friendly [1]. Due to the low humidity of the incoming air some of the water evaporates. This evaporation causes two favorable changes: a drop in the dry-bulb temperature and a rise in the relative humidity of the air. This non-saturated air cooled by heat and mass transfer is forced through enlarged liquid water surface area for evaporation by utilizing blowers or fans. Some of the sensible heat of the air is transferred to the water and becomes latent heat by evaporating some of the water. The latent heat follows the water vapour and diffuses into the air. In a DEC (direct evaporative cooling), the heat and mass transferred between air and water decreases the air dry bulb temperature (DBT) and increases its humidity, keeping the enthalpy constant (adiabatic cooling) in

an ideal process. However, 100% saturation is impossible for direct evaporative coolers due to two reasons [2]. Firstly, most of the pads are loosely packed or with cells, therefore the process air can easily escape between the pads without sufficient contact with the water. After water evaporates, it enters the air as water vapor and conveys the heat absorbed during evaporation back to the air in the form of latent heat. The effectiveness of this system is defined as the rate between the real decrease of the DBT and the maximum theoretical decrease that the DBT could have if the cooling were 100% efficient [1]. Practically, wet porous materials or pads provide a large water surface in which the air moisture contact is achieved and the pad is wetted by dripping water onto the upper edge of vertically mounted pads. According to [1] experimental studies are reliable and convincing; but they are usually costly and too tasking. In addition, the experiment results were obtained under various testing conditions with different type of pad materials which are affected by the environmental conditions with given inlet parameters and the results may be different when testing conditions is changed. Modeling analysis of evaporative cooling system is essential to explain the heat and mass transfer process in evaporative cooling and to predict the process outputs at various conditions. Over the years a number of

models have been developed with different pad materials to describe direct evaporative cooling systems, not supported with a heat exchanger [3, 4, 5, 6].

Most of these models ignore the thermal properties of the cooling pad material which will definitely affect the temperature drop inside the cooling chamber no matter how small. The models consider the heat and mass transfer that occur at the surface of the pad but in actual fact the cooling pad is a plain porous wall with thickness. Also the heat and mass transfer is not only on the surface but across the thickness with the air at the outer surface at different temperature from the air at the inner surface. Several materials have been used to provide the wet surface for air water contact. The major characteristic of these materials is that they were able to hold water and allow air to pass through. Several cooling pad materials tested under different climates include metal pads, cellulose pad, hessian pads, celdek, glasdek, PVC pad, porous ceramic pad, wood shaven, jute, rice straw; excelsior of pine, fir, cotton wool. Others are luffa, cedar, red wood, spruce, plain and etched glass fibers, copper, bronze, galvanized screening, vermiculite, perlite, expanded paper and woven plastic [1,7,8,9]. Most of these materials were evaluated under the temperate climate unlike the tropical climate with high solar load and high humidity most part of the year. With increasing market for active evaporative cooling systems, and the effort by researchers to adapt their performance to specific region, there is the need to investigate the possibility of using other local materials as cheaper alternative cooling pads. Krishpersad [10] has revealed that under tropical climate palm fruit fiber is good thermal insulator and preliminary investigation has shown that it has good water retention capacity, but review of literature shows that despite its abundance as a waste material in palm oil production, it has not been utilized in evaporative cooling system. The objective of the paper is to develop a mathematical model for direct evaporative cooling system incorporating the thermal properties and the thickness of the material of the pad (palm fruit fiber) in the heat and mass transfer process in a tropical environment and also presents wide range of heat transfer coefficient at the tested conditions.

**2. Basic Mathematical Model**

**2.1 Model assumptions**

- i. The system is adiabatic

- ii. The cooling pad is a plain porous wall bounded by two convective fluids (air) at different temperature.
- iii. The surface of the pad is completely wet
- iv. The cooling pad is rigid

**2.2 Basic model equation**

On the assumption that the cooling pad is a plain porous wall bounded by two convective fluids (air) outside the pad surface and inside the cooler, each at different temperature, the elementary sensible heat flux in terms of overall temperature and thermal properties of the pad for figure 1 is given by

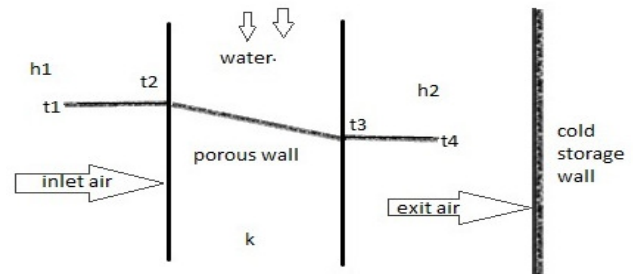


Figure 1: Scheme of the heat transfer process across the porous evaporative cooling pad

$$dq = h_1(T_1 - T_2)dA \tag{1}$$

$$dq = \left( \frac{T_2 - T_3}{\frac{x_{23}}{k_{23}}} \right) dA \tag{2}$$

$$dq = h_2A(T_3 - T_4)dA \tag{3}$$

The heat balance for the three equations gave

$$dq = \left( \frac{T_1 - T_4}{\frac{1}{h_1} + \frac{x_{23}}{k_{23}} + \frac{1}{h_2}} \right) dA \tag{4}$$

$h_1$  and  $h_2$  are the convective heat transfer coefficient,  $A$  is the area of the pad,  $k$  is the thermal conductivity of the pad,  $x$  is the thickness and  $T$  is the temperature

[11] gave the mass flow rate of re-circulating water evaporating into air from a surface in terms of the mass transfer coefficient for evaporative cooler as

$$\dot{\omega} + \left( \frac{\delta \dot{\omega}}{\delta A} \right) dA = \dot{\omega} + h_D(\omega_s - \omega)dA \tag{5}$$

He gave the simplified solution as

$$d\dot{\omega} = h_D(\omega_s - \omega)dA \tag{6}$$

$h_D$  is convective heat transfer coefficient,  $\omega$  is the humidity ratio,  $\dot{\omega}$  is the mass flow rate of water,  $A$  is the surface area of the cooling pad, subscript  $s$  is saturated moist air at water temperature

Based on equation 6 [6] stated that the water mass flow rate does not remain constant due to the process of evaporation. Simultaneous heat and mass transfer takes place at the air-water interface. [5] analyzed the interface of air - liquid of direct evaporative cooling system, by energy conservation and gave the heat passing through the air -water interface as

$$dq = m_a c_{pu} dT \tag{7}$$

Where  $C_{pu}$  is given by  $c_{pu} = c_{pa} + w c_{pv}$  (8)

$C_{pu}$  is the humid specific heat,  $c_{pa}$  is the specific heat of dry air,  $c_{pv}$  is the specific heat of vapour

Since the quantity of heat loss by draft air and the cooling pad is equal to heat passing through air-water interface. The overall energy balance on the process fluid and the cooling pad will be

$$\left( \frac{T_1 - T_4}{\frac{1}{h_1} + \frac{x_{23}}{k_{23}} + \frac{1}{h_2}} \right) dA = m_a c_{pu} dT \tag{9}$$

The above equation can be integrated resulting in

$$m_a c_{pu} \left( \frac{1}{h_1} + \frac{x_{23}}{k_{23}} + \frac{1}{h_2} \right) \int_0^A dA = \int_{T_1}^{T_4} \frac{dT}{T_1 - T_4} \tag{10}$$

The integration will yield

$$- \left[ \frac{A}{m_a c_{pu} \left( \frac{1}{h_1} + \frac{x_{23}}{k_{23}} + \frac{1}{h_2} \right)} \right] = in \left[ 1 - \frac{T_1 - T_4}{T_1 - T_w} \right] \tag{11}$$

In (11),  $\frac{T_1 - T_4}{T_1 - T_w}$  is the evaporative efficiency or effectiveness and is represented by  $\mathcal{E}$

With the hypothesis that air and vapor are perfect gases, [5] gave the enthalpy change as

$$h_g - h = C_{pu}(T_s - T) + h_{vs}(w_s - w) \tag{12}$$

Where  $h_{vs}$  is specific enthalpy of vaporization

Assuming that  $h_{vs} \approx h_{lvs}$  the above equation becomes

$$h_g - h = C_{pu}(T_s - T) + h_{ls}(w_s - w) \tag{13}$$

$h_{lvs}$  is the vapour enthalpy at the surface of the cooling pad.

However in the presence of difference in enthalpy the term  $h_{ls}(w_s - w)$  is neglected [12] therefore the change in enthalpy for the direct evaporative cooler can be written as

$$\Delta H = c_{pu} \Delta T \tag{14}$$

Therefore

$$\frac{\Delta H}{\Delta T} = c_{pu} \tag{15}$$

$$A = w \times L \tag{16}$$

$W$  and  $L$  is the width and length of the pad

Therefore

$$- \left[ \frac{wL}{\frac{\Delta H m_a \left( \frac{1}{h_1} + \frac{x_{23}}{k_{23}} + \frac{1}{h_2} \right)}{\Delta T}} \right] = in [1 - \mathcal{E}] \tag{17}$$

$$\mathcal{E} = 1 - \exp \left\{ - \left[ \frac{wL}{\frac{\Delta H m_a \left( \frac{1}{h_1} + \frac{x_{23}}{k_{23}} + \frac{1}{h_2} \right)}{\Delta T}} \right] \right\} \tag{18}$$

The convective heat transfer is calculated from the nusselt number as follows

$$N_U = \frac{hl}{k} \tag{19}$$

Where  $k$  is the thermal conductivity of air,  $l$  is the characteristic length and is given by [5] as

$$l = \frac{\ell}{A} \tag{20}$$

Where  $\ell$  is the volume occupied by the pad.

[13] gave a correlation to determine the heat transfer coefficient for a rigid evaporative media as

$$N_U = 0.1 \left( \frac{l}{x} \right)^{0.12} R_e^{0.8} Pr^{\frac{1}{3}} \tag{21}$$

Where the Reynolds number  $R_e$  is given by

$$R_e = \frac{vl}{\nu} \tag{22}$$

where  $v$  is the air speed,  $\nu$  is the kinematic viscosity

also the Prandtl number  $Pr$  is given by

$$Pr = \frac{\nu}{\alpha} \tag{23}$$

Where  $\alpha$  is the thermal diffusivity which is given by

$$\alpha = \frac{k}{\rho c_{pa}} \tag{24}$$

Where  $\rho$  is the density of air and  $c_{pa}$  is the specific capacity of air.

The mass flow rate was generated from the continuity equation as follows

$$m_a = \rho A_1 v \tag{25}$$

where  $A_1$  is the area of the pad covered by each of the three fan since the pad is divided into three compartments.

### 2.3 Experimental Tests

An experimental test was conducted with palm fruit fiber as the cooling pad material at inlet air velocities of 4.0 m/s and exit speed of 1.6m/s. The characteristic length of the pad is 0.3 with a height of 1m. The pad was divided into three equal area with each mounted with an axial fan delivering 0.5kg/s of air at a pad face velocity of 1.6m/s. The test facility figure 2 was located under an open shade built under a whistling pine tree. This is to reduce direct action of the sun and expose the cooler to natural air. The test was carried out in January and February of 2013; this period presented the extremes of the temperature within the year. At this period, there was rain for 8 days, which presented very high ambient relative humidity of 80 %. In addition, the period presented extreme low humidity of 28 % and very high temperature of 45 °C. The palm fruit fiber was loaded into the pad holder at a thickness of 30mm and a parking density of 20 - 22 Kg /m<sup>3</sup>. The upper water tank delivers water at a rate of 10 cm<sup>3</sup>/s. The water flows through the pad by gravity into the bottom tank and re-circulates back with the water pump. The cooler is loaded with 2 kg of pumpkin (cucurbita) and amaranthus. A thermocouple (omega data logger, HH1147) ( $\pm 0.1$  °C) was positioned through the hot wire terminals inserted into the cooling chamber. One of the terminals was covered with cotton wool soaked inside the water to measure the wet bulb temperature [14]. The air speed of the fan was determined with vane microprocessor (AM-4826) digital anemometer ( $\pm 0.1$ m/s). Two ABS temperature and humidity clock ( $\pm 0.1$  °C and 1.0 %) was positioned inside the

shade and another outdoor where there is no shade to record the temperature and humidity of the ambient. Two analogue thermometers were inserted inside the two tanks to measure the water temperature. The data were logged every two hours. The relative humidity and the enthalpy of the cooler were obtained from the psychrometric chart. In addition, the wet bulb temperature and the enthalpy of inside the shade and the ambient were calculated also from the psychrometric chart.

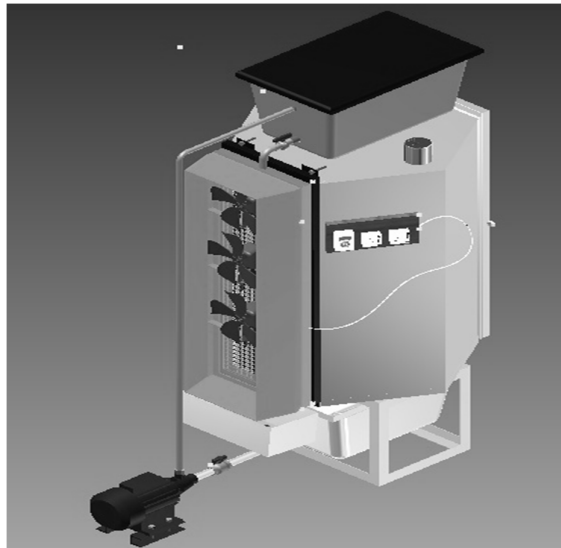


Figure 2: schematic evaporative cooling system test rig

**2.4 Performance Evaluation**

The cooling efficiency defined by Equation 1 is a widely used index for evaluating the performance of direct evaporative cooling systems [15, 16]. They were used as follows:

Cooling efficiency ( $\ell$ )

$$\ell = \frac{T_{db} - T_s}{T_{db} - T_w} \tag{26}$$

$\ell$  is the cooling efficiency;  $T_{db}$  is the dry bulb temperature of the ambient air;  $T_s$  is the dry bulb temperature of the cold air inside the cooling chamber;  $T_w$  is the wet bulb temperature of the ambient air.

**3. Results and Discussion**

**3.1 Model validation**

The mathematical model was validated using data generated from an existing active evaporative cooler figure 2. The model validation was done at a constant draft air mass flow rate of 0.5kg/s and exiting air speed of 1.6m/s at a constant pad thickness of 30mm and water flow rate of 10cm<sup>3</sup>/s. In the first day the ambient temperature ranged from 29.9 – 34.8°C with a relative humidity of 34 – 51% while it ranged from 26.1- 34°C for the second day with a relative humidity of 38 -69%. Also at the third day the ambient temperature ranged from 27.8 -34 °C while the relative humidity ranged from 44 – 73%. At these prevailing environmental condition the cooler maintained a temperature range of 23.2 -24.8°C with a relative humidity of 90.4 -94.8% on the first day while on the second day it provided a cooler temperature of 23.2- 24.6°C with a relative humidity of 93.6 – 96.8%. On the third day the ambient condition provided a cooler temperature of 23.8 – 25.2°C with a relative humidity of 85.6 -96.8%. The evaluation parameters (table 1-7) were fitted into equation 18 to calculate the predicted cooling efficiency while the experimental efficiency was calculated with equation 25.

Table 1: evaluation parameters

Evaluation Parameters								
day one			day two			day three		
Time(hr)	ΔH	ΔT	Time(hr)	ΔH	ΔT	Time(hr)	ΔH	ΔT
10	2.05	4	10	2.9	6	9	1.54	2.9
12	0.4	6.5	11	6.58	6.7	11	2.37	4.8
14	5.05	9.7	12	4.99	8.2	13	2.04	7.4
16	0.18	8.2	13	5.08	9	15	2.12	9.7
18	4.51	7.7	16	3.42	10	17	6.74	8.7
			18	7.5	8.3			

Table 2. Calculated properties of the draft at day one

Time (hrs)	Cold air properties								
	Tdc (°C)	V × 10 <sup>-6</sup> (m/s)	P (Kg/m <sup>3</sup> )	C <sub>pa</sub> (kj/kg.K)	k (W/m.K)	Re	P <sub>r</sub>	Nu	h2(W/m <sup>20</sup> K)
9	23.2	15.41	1.193	1.005	0.0260	3115	0.713	557	483
11	24.2	15.50	1.189	1.005	0.0260	3096	0.713	557	483
13	24.2	15.50	1.189	1.005	0.0260	3096	0.713	554	480
15	24.3	15.53	1.188	1.005	0.0260	3090	0.713	554	480
17	24.6	15.54	1.187	1.005	0.0260	3089	0.713	553	479

Table 3. Calculated properties of cold air at day one

Time (hrs)	Draft air properties								
	Tdb (°C)	V × 10 <sup>-6</sup> (m/s)	P (Kg/m <sup>3</sup> )	C <sub>pa</sub> (kj/kg.K)	k (W/m.K)	Re	P <sub>r</sub>	Nu	h1(W/m <sup>20</sup> K)
9	26.1	16.28	1.181	1.005	0.0261	7371	0.712	1108.9	964.7
11	29	15.95	1.170	1.005	0.0263	7524	0.712	1103.3	967.2
13	31.6	16.19	1.160	1.005	0.0265	7411	0.712	1113.7	983.8
15	34	16.41	1.150	1.005	0.0267	7411	0.712	1113.7	983.8
17	33.3	16.35	1.153	1.005	0.0266	7339	0.712	1105	979.8

Table 4. Calculated properties of draft at day two

Time (hrs)	Draft air properties								
	Tdb (°C)	V × 10 <sup>-6</sup> (m/s)	P (Kg/m <sup>3</sup> )	C <sub>pa</sub> (kj/kg.K)	k (W/m.K)	Re	P <sub>r</sub>	Nu	h1 h2(W/m <sup>20</sup> K)
10	29.9	16.03	1.166	1.005	0.0264	7486	0.712	1123	988.24
11	30.3	16.07	1.165	1.005	0.0264	7467	0.712	1120	985.6
12	31.4	16.17	1.161	1.005	0.0265	7421	0.712	1114.9	984.82
13	32.8	16.30	1.155	1.005	0.0266	7362	0.712	1107.8	982.4
14	33.4	16.36	1.153	1.005	0.0266	7335	0.712	1104.6	979.4
16	34.8	16.49	1.153	1.005	0.0267	7277	0.712	1097.6	986.9
18	32.6	16.28	1.156	1.005	0.0266	7371	0.712	1108.9	983.22

Table 5. Calculated properties of cold air at day two

Time (hrs)	Cold air properties								
	Tdc (°C)	V × 10 <sup>-6</sup> (m/s)	P (Kg/m <sup>3</sup> )	C <sub>pa</sub> (kj/kg.K)	k (W/m.K)	Re	P <sub>r</sub>	Nu	h2(W/m <sup>20</sup> K)
10	23.9	15.47	1.190	1.005	0.0260	3103	0.713	555	481
11	23.6	15.44	1.191	1.005	0.0260	3109	0.713	556	482
12	23.2	15.41	1.193	1.005	0.0260	3115	0.713	557	483
13	23.8	15.46	1.193	1.005	0.0260	3105	0.713	556	482
14	25.2	15.59	1.185	1.005	0.0260	3078	0.713	551	478
16	24.8	15.56	1.186	1.005	0.0261	3085	0.713	552	478
18	24.3	15.51	1.188	1.005	0.0260	3095	0.713	554	480

Table 6. Calculated properties of the draft and cold air at day three

Time (hrs)	Draft air properties								
	Tdb (°C)	V × 10 <sup>-6</sup> (m/s)	P (Kg/m <sup>3</sup> )	C <sub>pa</sub> (kj/kg.K)	k (W/m.K)	Re	P <sub>r</sub>	Nu	h1(W/m <sup>20</sup> K)
10	27.8	15.84	1.175	1.005	0.0262	7575	0.712	1128.6	985.6
12	30.3	16.07	1.165	1.005	0.0264	7467	0.712	1120.5	986
14	33.8	16.39	1.151	1.005	0.0267	7321	0.712	1102.9	981.6
16	34	16.41	1.150	1.005	0.0267	7411	0.712	1113.7	991.2
18	31.9	16.22	1.159	1.005	0.0265	7398	0.712	1112.2	982.4

Table 6. Calculated properties of cold air at day three

Time (hrs)	Cold air properties								
	Tdc (°C)	V × 10 <sup>6</sup> (m/s)	P (Kg/m <sup>3</sup> )	C <sub>pa</sub> (kJ/kg.K)	k (W/m.K)	Re	P <sub>r</sub>	Nu	h <sub>2</sub> (W/m <sup>20</sup> K)
10	23.8	15.46	1.190	1.005	0.0260	3105	0.713	555	481
12	23.8	15.44	1.190	1.005	0.0260	3109	0.713	556	482
14	24.1	15.49	1.189	1.005	0.0260	3099	0.713	554	480
16	25.8	15.65	1.182	1.005	0.0261	3067	0.713	550	477
18	24.2	15.50	1.189	1.005	0.0260	3097	0.713	554	480

ΔH is change in enthalpy, ΔT is change in temperature.

Also air properties determined from psychometric chart were fitted into equation 19 – 23 to calculate the coefficient of heat transfer for the two air conditions (table 1-6). Thermal conductivity of palm fiber was 0.057W/m<sup>20</sup>K [10]. The air properties determined from the relevant equation cited in the model procedure for a typical consecutive three day period is presented in table 1-7. The predicted and experimental cooling efficiency is presented in fig 3- 5.

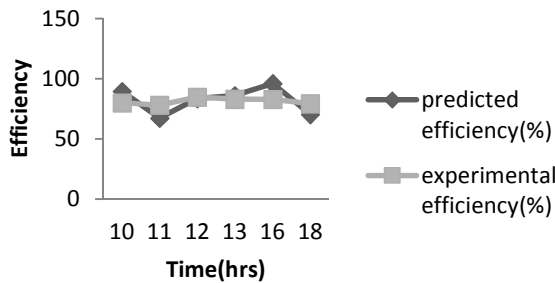


Figure 3: Hourly predicted and experimental cooling efficiency (%) for day one.

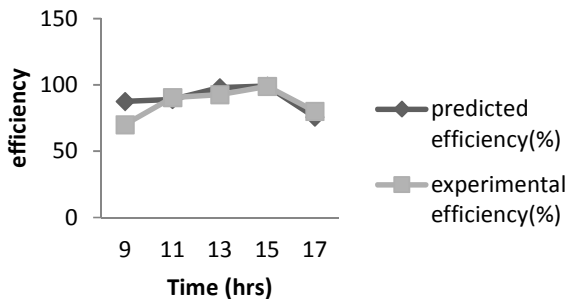


Figure 4: Hourly predicted and experimental cooling efficiency (%) for day two.

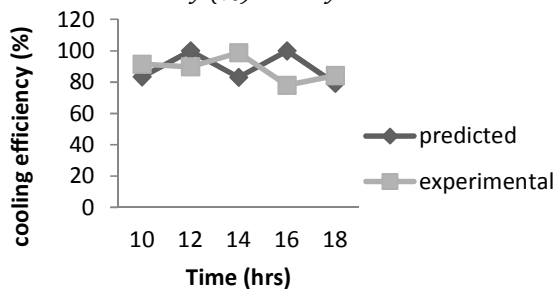


Figure 5: Hourly predicted and experimental cooling efficiency (%) for day three.

In order to be certain there is difference in the predicted and experimental efficiency; analysis of variance was performed on the results of the three days of test. The F – value shows that there was no significant difference at the 5% level. The average mean efficiency difference on the first day for cooling efficiency and the predicted efficiency was 0.8% while the second day gave average mean difference of 3.45%. Also the third day gave an average mean difference of 3.72%. These values are very close to the experimental values as shown in figure 6

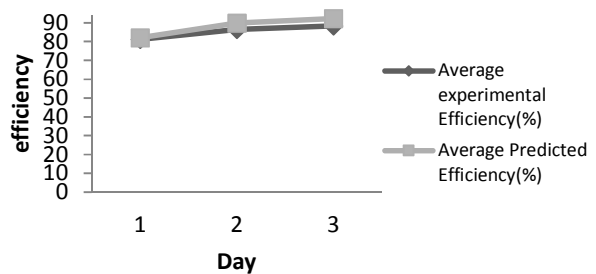


Figure 6: average daily experimental and predicted efficiency

This shows that the model have close to 96 – 99.2% accuracy. The convective heat transfer shows a decrease with increase in temperature as shown from tables 1- 6 and the range falls within the range calculated for inlet temperature of the same range which agrees with several work in literature [17] Figure 2 and 5 showed that the model performed relatively poorly at 16hrs for the two days period compared to the rest of the period. This might be because 16hrs is mostly the transition point where the temperature gradient of the cooler starts to decrease. The best fit equation for the experimental and predicted value is given by

$$pre(\mathcal{E}) = -2.745\exp(\mathcal{E})^2 + 16.03 \exp(\mathcal{E}) + 68.76 \quad (26)$$

The above equation has R<sup>2</sup> value of 100% The value of the Reynolds number at the inlet shows that the air is turbulent (Re > 5000) which is typical of force convection. Though the air enters into the cooling pad as a turbulent flow but it emerges as a laminar flow inside the cooling

chamber ( $Re < 5000$ ) as shown in table 1-6. This shows that the cells of the cooling pad absorb some of the energy from the air.

### 5. Conclusion

The equation for predicting the cooling efficiency of a direct evaporative cooler for storage has been presented and validated. The model considered the thermal conductivity and thickness of the cooling pad material. The model has 96 – 99.2% accuracy. The information presented could be useful in the design of evaporative cooling for other purposes.

### References

1. Xuan Y.M. ; F. Xiao; X.F. Niu; X. Huang ; S.W. Wang. Research and application of evaporative cooling in China: A review, *Renewable and Sustainable Energy Reviews* Volume 16, Issue 5, June , 2012, pp 3535 - 3546
2. Di Y.H., J.P. Liu, X. Huang . Climate demarcating for application of evaporative cooling air conditioning. *HVAC*, 40 (2) , 2010, pp. 108–111
3. Al-Helal I and Short T H. A CFD study of naturally and ventilated greenhouses in extreme arid climates. *ASAE Paper* no. 99-5011, 1999
4. Liao, C.; Chiu, K. Wind Tunnel Modeling the System Performance of Alternative Evaporative Cooling Pads in Taiwan Region. *Building and Environment*. 2002., p. 177-187
5. Camargo J. R., C. D. Ebinuma, S. Cardoso, a mathematical model for direct evaporative cooling air conditioning system: *Engenharia Térmica*, nº 4, 2003, p. 30-34
6. Qiang T. W., H .G. Shen, J. M. Feng, R.J. Liang Application of direct evaporative cooling air conditioning in moderate and high humid area of china. *Refrigeration and Air-conditioning*, 27 (3) 2006, pp. 21–25
7. Al-Sulaiman, F. Evaluation of the Performance of local Fibers in Evaporative Cooling. *Energy Conversion and Management*, 43, 2002, 2267-2273
8. Manuwa S. I. and S. O. Odey . Evaluation of Pads and Geometrical Shapes for Constructing Evaporative Cooling System. *Modern Applied Science*; Vol. 6(6), 2012, pp 45-53
9. Darwesh, M, Abouzaher, S., Fouda, T., & Helmy, M.. Effect of Using Pad Manufactured from Agricultural Residues on the Performance of Evaporative Cooling System. *Jordan Journal of Agricultural Sciences*, 5(2), 2009, 111-125.
10. Krishpersad.M. Renewable building thermal insulation-oil palm fiber. *International journal of engineering and technology*. Pp 475-479(2) 2012.
11. Qureshi B. A., Zubair M. A comprehensive design and rating study of evaporative coolers and condensers. Part I. Performance evaluation: *International Journal of Refrigeration*, 29, 2006, pp 645–658
12. El-dessouky .H. T., H. M. Ettouney and W. Bouhamra, A novel air conditioning system membrane air drying and evaporative cooling. *Trans IChemE, Vol. 78, Part A*, 2000, pp 999- 1009
13. Dowdy, J. A.; Karabash, N. S.. Experimental Determination of Heat and Mass Transfer Coefficients in rigid Impregnated Cellulose Evaporative Media. *ASHRAE Transactions*, part 2, vol. 93. 1987, pp. 382-395.
14. Anyanwu E.E. Design and measured performance of a porous evaporative cooler for preservation of fruits and vegetables. *Energy conversion and management* ,45, 2004, 2187–2195
15. Jain. D. Development and testing of two-stage evaporative cooler .*Building and Environment*, (42), 2007, 2549–2554.
16. Ndukwu, M. C. Development of Clay Evaporative Cooler for Fruits and Vegetables Preservation. *Agricultural Engineering International: CIGR Journal*, 13(1), 2011, 1-8.
17. Ditchfield .C; C.C. Tadini; R.K Singh; R.T. Toledo. Velocity and temperature profile, heat transfer coefficient and residence time distribution of temperature dependent Herschel bulky fluid in tubular heat exchanger. *Journal of Food Engineering* (79), 2006, 632 -638